Available online at www.CivileJournal.org

Civil Engineering Journal

(E-ISSN: 2476-3055; ISSN: 2676-6957)

Vol. 8, No. 11, November, 2022

Performance Flexural of RC Beams Without Concrete at Tension Cross-section

Astiah Amir [1*], Aulia Rahman [1], Lissa Opirina [1], Fadli Idris [1]

[1] *Department of Civil Engineering, Faculty of Engineering, Teuku Umar University, Meulaboh, Indonesia.*

Received 12 August 2022; Revised 06 October 2022; Accepted 19 October 2022; Published 01 November 2022

Abstract

This study aims to analyze the flexural capacity of RC without concrete in a tension cross-section using an experimental method. The number of specimens is three pieces, namely a spiral reinforced concrete beam (SBC) and a vertical reinforced concrete beam (CBN); both of these blocks are without concrete in the cross-section of the reinforcement and 60D tensile steel reinforcement in the support area, where D is the primary diameter, and a conventional concrete beam as the control beam (CB). The beam size is 3100×150×200 mm. The beams are supported by simple supports with a span of 3000 mm. The concrete in the structural beam elements, which work optimally to withstand the load, is the outermost fibre part of the side, while the concrete on the tension side does not have a direct role in determining the magnitude of the resisting moment. Therefore, the quality of the concrete in the concrete beam section must be optimized, while the concrete in the tension section must be minimized. Eliminating concrete in tension areas reduces the construction's self-weight and use of concrete-making materials. The main variables in this research are bending behaviour and crack pattern. The beam specimens were tested with two-point loading monotonically. By observing the crack pattern and failure mode, the results showed an increase in the capacity load of SBC by 21.58% CBN but a decrease of 27.57% compared to the CB control beam. Flexural cracks and beam failures resembled under-reinforcing. The flexural capacity was analyzed based on static analysis and then validated by calculating the ratio between the theoretical nominal moment and the experimental moment. This finding shows that changing the conventional shear reinforcement model to spiral can increase the flexural of the beam without concrete in the tension cross-section.

Keywords: Flexural Capacity; Spiral Reinforced; Tensile Cross-Section; Tensile Reinforcement.

1. Introduction

Concrete is a building material that is still very popular in the construction industry. In addition to its high workability, it is also easy to maintain and has a long economic life. However, the ingredients for this concrete mix use materials from nature, such as gravel, sand, and cement, so their fulfillment results in natural exploitation that impacts the environment. Various ways have been done to minimize these natural materials, which is in line with Gerges et al. [1], Prabha et al. [2], and Elsayed et al. [3]; Concrete can withstand compressive flexural stresses but has the disadvantage of resisting tensile stresses, so reinforcing steel is needed to withstand these tensile stresses. The magnitude of the resisting moment is affected by the concrete in the compression area.

Conversely, the concrete in the tension area does not play an important role in determining the magnitude of the resisting moment, so the concrete on the tensile side can be used with lower quality concrete or all the concrete on the tensile side can be removed. Reducing the volume of concrete is intended to make construction lighter and more economical. As illustrated in Figure 1. According to Whitney, the assumed uniform compressive stress of 0.85f'c is

* Corresponding author: astiahamir@utu.ac.id

http://dx.doi.org/10.28991/CEJ-2022-08-11-014

uniformly distributed over the equivalent compression region bounded by the cross-sectional edge of a straight line parallel to the neutral axis at a distance a = β1.c of the concrete fibres subjected to the compressive strain maximum εc. An equivalent rectangular press block can be used to calculate loads without loss of accuracy. Equivalent compression concrete withstands the compressive load on the compression side, while the concrete on the tensile side is considered non-functional because the tensile stress is resisted by the steel reinforcement, as shown in Figures 1 and 2.

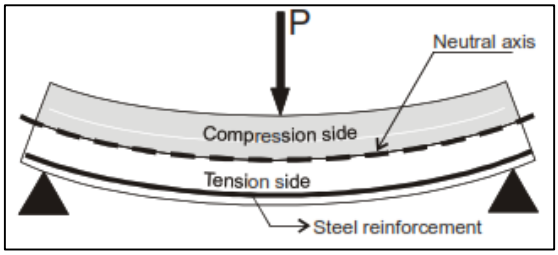

Figure 1. Compression-tension of a flexural beam

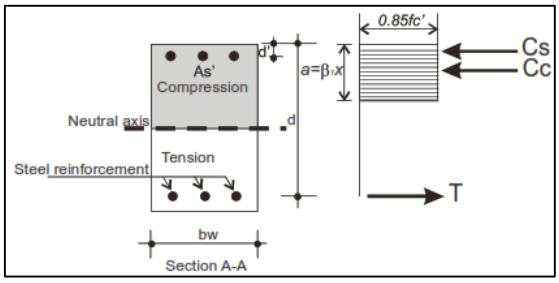

Figure 2. Rectangular stress block

Research on removing concrete in the tensile area in this spiral reinforced concrete beam has never been done before. Other studies generally minimize the use of concrete constituents by using cavities, replacing coarse aggregate with lightweight aggregate or hybrid concrete blocks, and using lower-strength concrete in tensile sections with or without replacing coarse aggregate with lightweight aggregate. In recent years, several studies have been carried out to reduce the use of concrete in construction, especially for beam sections [4], reporting a reduction in concrete in tension zones of up to 25%, and making hollow beams using GI pipes would be economical. The flexural strength of the RC hollow beam is almost the same as that of the RC control beam [5-7]; in another study, regarding the optimization of structural materials, Manikandan et al. [8] introduced hollow-core to the use of Expanded Polystyrene Foam in the zone tensile strength in RC beams, Patel [9] using hollow balls in reinforced concrete beams, obtained a weight reduction of about 12% and 33% of the crack and rupture index which is higher than that of control beam beams; furthermore, several studies on hybrid beams, layer on the tensile zone uses lower quality than concrete in the compression zone, by Ataria and Wang [10], Syahrul et al. [11], Fakhruddin et al. [12] and Hussein et al. [13] the results show the same thing, namely the hybrid beam has decreased flexural capacity.

Reducing the concrete in this tension section causes a decrease in the flexural capacity of the beam. This is in line with research Djamaluddin [14], so Amir et al. [15] has continued research by adding tensile reinforcement with a channel length of 60D in the support area of reinforced concrete beams from the truss system, the result of which is an increase in flexural capacity, and cracks and in the support area does not happen again. Research on the reinforcement of the frame system, Increase the shear strength of the beam and compressive reinforcement, tensile reinforcement requires shear reinforcement with several variations of geometric models, namely vertical, conventional system, truss system and spiral, for more details, as shown in Figure 3 [16-18].

(a) Conventional reinforcement (b) Spiral reinforcement

Figure 3. (a) Conventional reinforcement, (b) spiral reinforcement

Several research studies have shown that they can increase the flexural capacity of the beam [19, 20]. Conventional shear reinforcement, which functions to withstand bending moment loads, is converted into spiral reinforcement installed continuously on the axis of the concrete block and acts as reinforcement to withstand shear forces. Research related to spiral reinforcement is described by Ibrahim et al. [21], Askandar and Mahmood [22], Ibrahim et al. [23], and Al-Faqra et al. [24]. The change of vertical shear reinforcement into spiral shear reinforcement in beams is considered to increase the flexural capacity; according to Shatarat et al. [25], the shear capacity of SCC beams reinforced with rectangular spiral reinforcement is higher than traditional shear reinforcement regardless of the distance and angle of inclination for the stirrups. The increase in shear capacity ranges from 0.58% - to 16.27% for a stirrup spacing of 200 mm and 9.375% to 16.37% for a length of 150 mm. Furthermore, in another study of spiral-reinforced beams [26], spiral shear reinforcement reduced the occurrence of energy dissipation and increased flexural capacity and flexibility.

This study is presented in Section 2.1 describes the specimen and design of materials and introduces the material property. Section 2.2 Testing procedure, the beams testing is carried out with two-point loads on concrete blocks using monotonic loading, which is given displacement control with a constant ramp actuator speed of 0.03 mm / s until the beam collapses compares the test results depending on the test variables of the reinforcement types, failure modes, and reinforcing degree. Section 2.3 compares the load-deflection curves depending on the test variables. Section 3 summarizes the test results and findings. The research flow for this experimental study is shown in Figure 4.

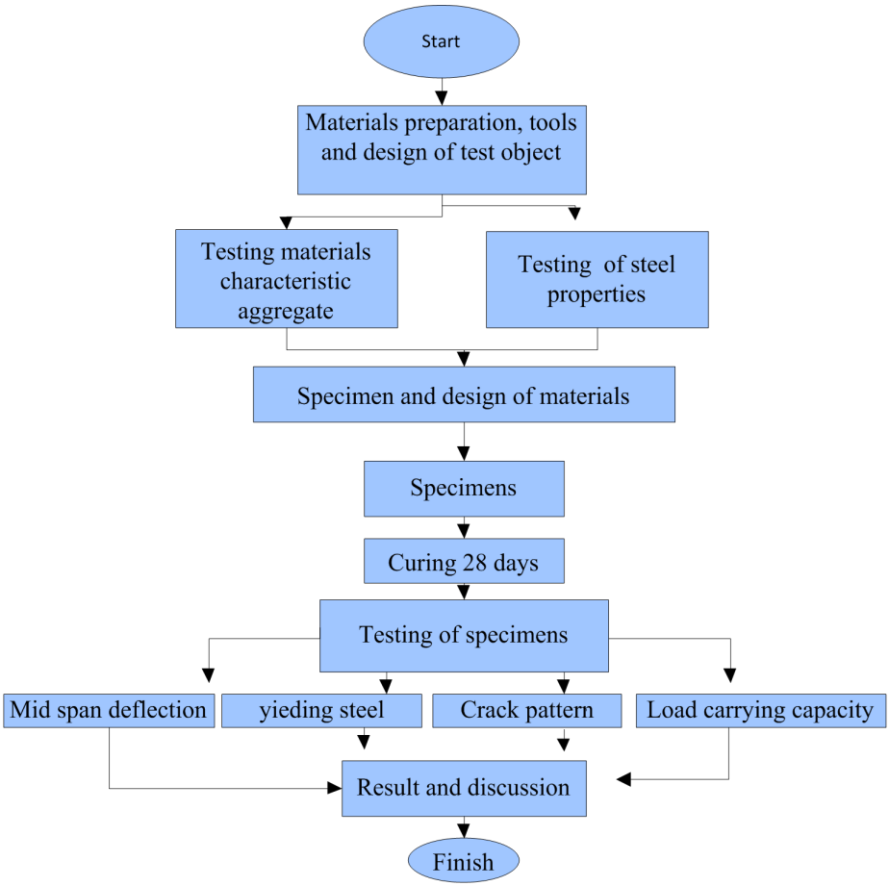

Figure 4. Flowchart of the research methodology

2. Experimental Program

The method used in this research based on the ASTM (American Society for Testing of Materials) and ACI (American Concrete Institute) regulations.

2.1. Specimens and Design of Materials

2.1.1. Specimen

A concrete mix design of normal concrete beam [27]. The design of concrete compressive strength was 45.07 MPa. The concrete beam variations to be studied are three specimens, each consisting of 1 (one) regular concrete block (CB), 1 (one) spiral reinforced concrete block, and 1 (one) conventional reinforced concrete beam; these two blocks are without concrete at the intersection of tensile with the strengthening of the tensile reinforcement rod in the 60D-long support area. The beam size is 3100 ×150 × 200 mm, as shown in Figure 5.

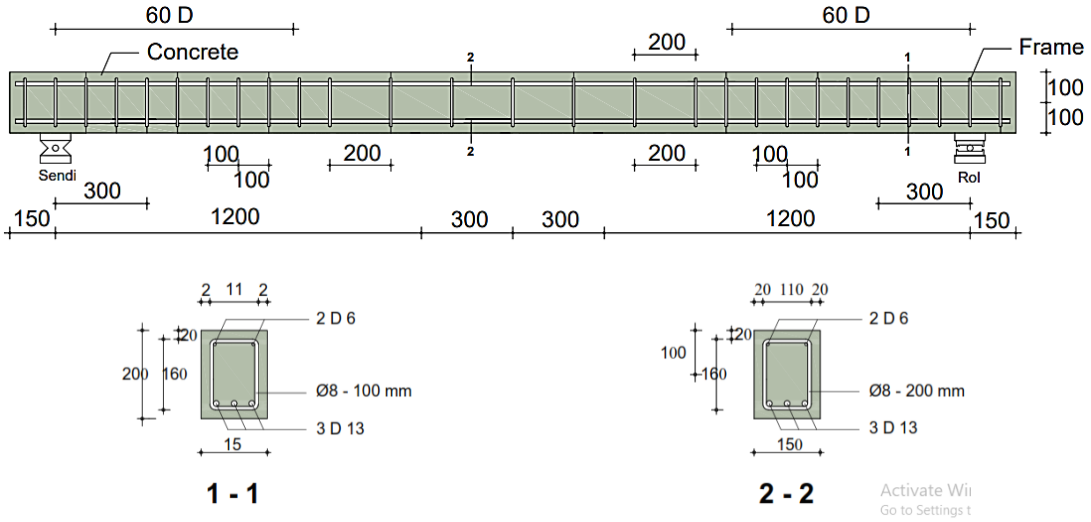

(a) Control Beam (CB)

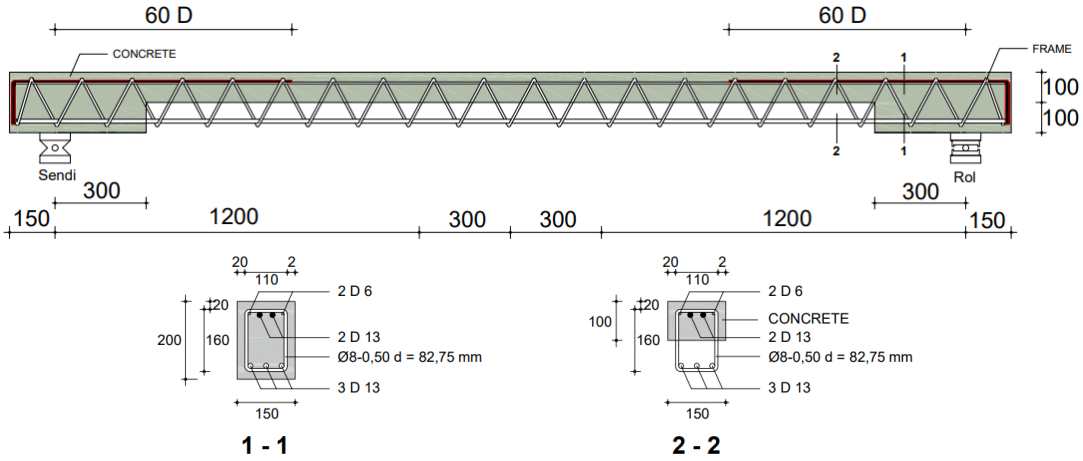

(b) Spiral Reinforced Concrete Beam without concrete on tensile cross section (SCB)

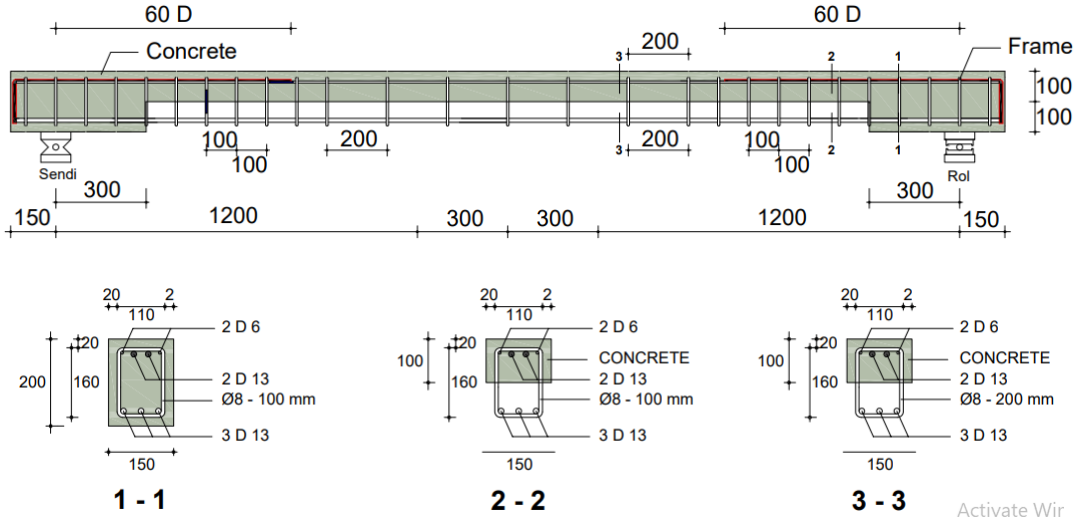

(c) Conventional reinforced concrete block without concrete on tensile cross section (CBN)

Figure 5. (a) CB Beam, (b) SCB Beam, (c) CBN Beam

2.1.2. Property Materials

Steel Material Testing

Plain steel material Ø8 mm, type Bj.TP 24, and threaded steel D13, type Bj.TS 24 where L_o = 300 mm, measured before the test; Also, is the original cross-sectional area of the test object; do is the cross-sectional area measured after testing; m is the required test object free length of 4 mm; it is the total length of the test object; and it is the length of the test object part wedged in the tensile machine. Concrete testing drawings and steel specimens can be seen in Figure 6.

Figure 6. Steel property testing

Concrete Material Testing

Specimens in the experimental program were prepared using ASTM. Type I Portland cement with a grade of 52.5 N/mm2. Natural clean sand was used as fine aggregate, while natural clean crushed dolomite stone was used as coarse aggregate (Size #1 and Size #2). Physical and mechanical properties of both fine and coarse aggregates were obtained by testing a set of random samples according to the ASTM C33 specification standards [28], the material used is fresh concrete used in slump testing and compressive strength. The cylinder samples were prepared according to ASTM C39-03 [29], The grading of coarse and fine aggregates is shown in Figure 7-a Gradation of Coarse Aggregate and Figure 7-b Gradation fine Aggregate, and upper, lower limit of ASTM C33.

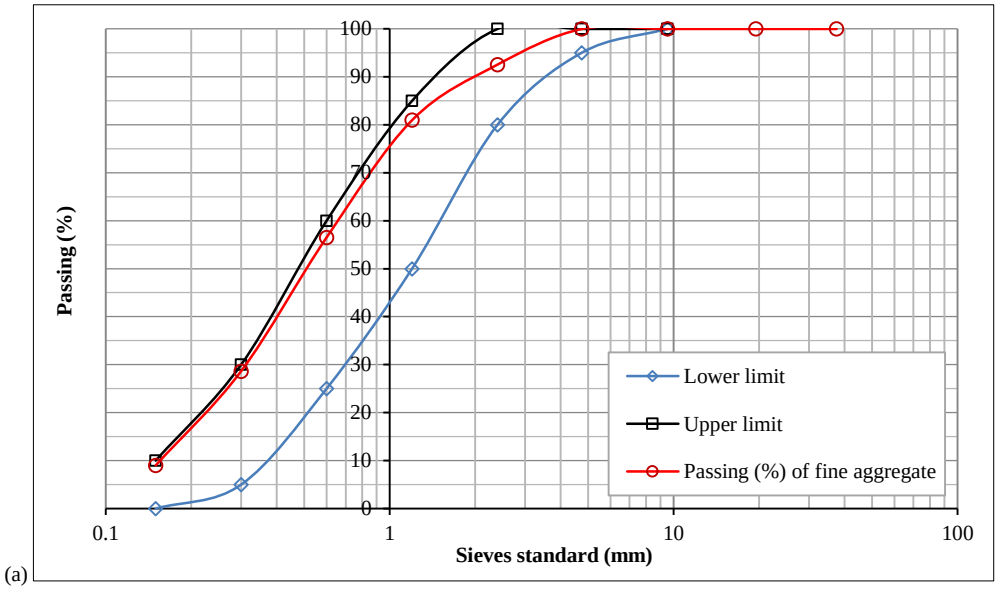

(a)

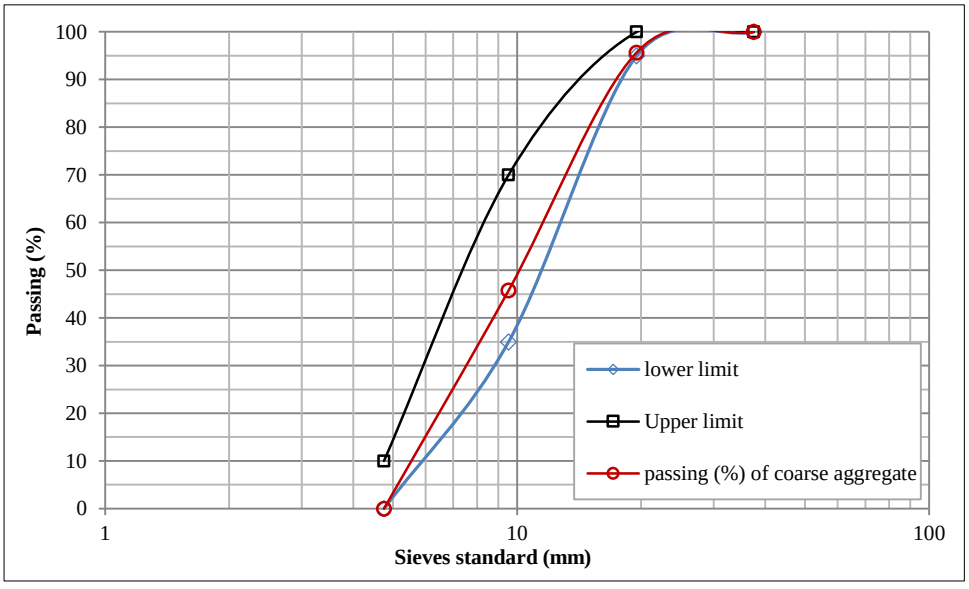

(b)

Figure 7. a) Gradation test of Coarse Aggregate, b) Gradation test fine aggregate, and Upper, and lower limit of ASTM C 33

The dimensions of the cylinder test object are 100 mm in diameter with a height of 200 mm. Concrete press strength testing is carried out after 28 days, and Concrete mixture testing can be seen in Figure 8.

Figure 8. Concrete property test

The results of the concrete and steel properties test can be seen in Table 1.

Table 1. Concrete and Steel Property Test Results

Concrete		Steel	
Compressive strength (*f'c*)	45.07 MPa	Yield Strength (fy)	365.14 MPa
Tensile strength (ft)	3.0 MPa	Ultimate strength (FS maks)	469.24 MPa
Flexural strength(fr)	33.64 MPa	Modulus of elasticity (Ɛs)	198890 MPa
Modulus of elasticity(Ec)	31.550 × 10^3 MPa	Yield Strain of stell (Es)	0.00199

2.2. Testing Procedure

The Beams testing is carried out with two-point loads on concrete blocks using monotonic loading, which is given displacement control with a constant ramp actuator speed of 0.03 mm /s until the beam collapses. The data reading on the logger is taken at each increase in lending under normal conditions. This test aims to obtain data on the maximum load the beam can withstand, strain, and deflection that occurs. Steel and concrete stretching and tensions will be monitored for any 100 kg load increase using LVDT (transducer) tools and gauge strains. LVDT is placed at 3 locations on one beam; steel gauge strains are identified as shear reinforcement and compressive reinforcement, while concrete gauge strains are placed in the middle of the span, as shown in Figure 9.

Figure 9. Loading Test

3. Results and Discussions

3.1. Load-Deflection Relation

Figure 10 presents the specimen load-deflection relationship graph measured at the center of the beam. The first crack occurs, indicating that the moment that occurred exceeded the capacity of the crack moment in the beam. The first crack causes a decrease in stiffness in the beam, but in the first crack of the CBS beam, CBN does not cause a significant reduction in the deflection slope of the load as in a control beam. The first crack in SCB occurs when a load of 3.33 kN with a deflection of 1.81 mm is applied, while the first crack in CBN occurs when a load of 2.06 kN with a deflection of 1.91 mm is applied. When a load of 4.11 kN with a deflection of 2.15 mm is applied, control beams are the first to crack. The first crack load on the SCB beam is higher than the CBN beam, and the deflection is lower, but compared to the control beam (CB), the first two crack beams of both rays are lower. This shows that the beam does not yet have tenacity in the elastic phase compared to the control beam. This is made possible by the decrease in inertia due to the reduction of concrete in the tensile cross-section, resulting in a 46% reduction in inertia compared to the control beam (CB). Changing the vertical shear reinforcement model to a spiral to increase the Pcr value is insignificant. Still, the influence of the spiral system can be observed when the primary reinforcement has melted the difference in yielding load (*py*) and ultimate load (Pu).

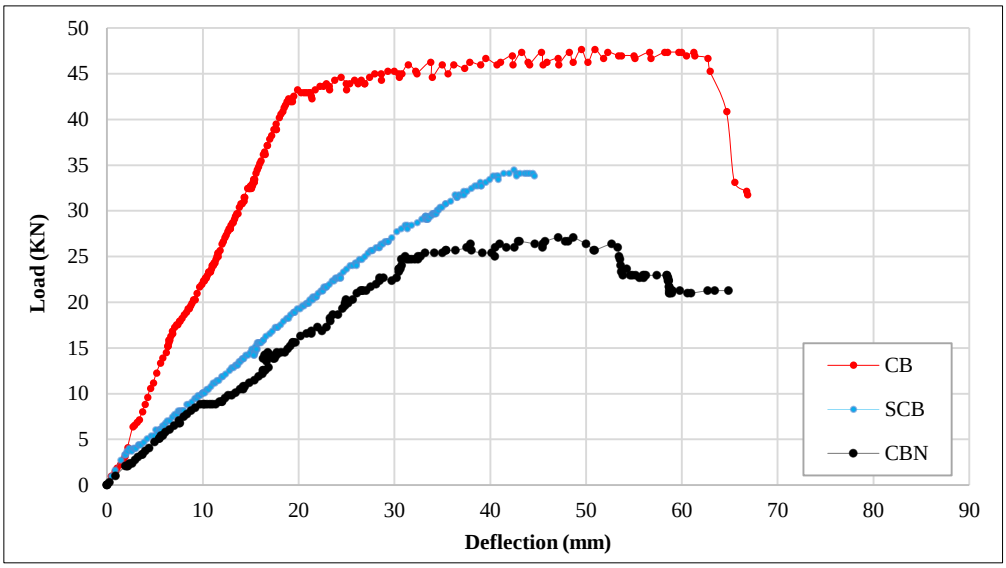

Figure 10. Load-deflection of the beams

Behavior deflection of the specimen control beam (CB), judging by the deflection of the curve load, the control beam curve is more upright than the SCB and CBN specimens. It can be seen in the load and deflection relationships on the SCB and CBN beams with limited conditions before the bending collapse of the specimen according to the initial cracking stage, melting. This means that CB specimens are stiffer than SBC specimens, and SBN specimens, but SBC specimens are stiffer than SBN specimens. Likewise with the ultimate load, which affects the nominal moment, calculation of the ultimate moment capacity through the use of the Equation 1.

$$Mu_{cal} = A_{sfy}(d - 0.5a) \quad (1)$$

The relation of deflection load from the specimen test results of the load under initial crack conditions, ultimate load, maximum deflection and the moment that occurred using moment holding formula is presented in Table 2.

Table 2. Result of Loading Test and Analysis calculated of Moment crack, yield, and ultimate

Description	Unit	Specimen Beams					
		CB	SCB	CBN	CB	SCB	CBN
		Analysis			Experimental		
Pcr	kN	4,48	4,48	4,48	4.11	3.33	2.06
Mcr	kNm	3,50	3,50	3,50	3.27	2.81	2.05
Py	kN	33,37	33,37	33,37	41.96	33.82	25.68
Mpy	kNm	20,83	20,83	20,83	25.98	21.1	16.22
Pu	kN	35,75	35,75	35,75	47.65	34.51	27.06
Mu	kNm	22,26	22,26	22,26	29.39	21.52	17.05
Mu_{exp}/Mu_{Cal}					1.30	0.97	0.8
Maximum deflection (Midspan)		33.86	44.91	44.91	49.49	42.47	42.51

While theoretical Maximum deflection (Midspan) is calculated using of the Equation 2.

$$\delta = \frac{Pa}{48\ Ec.Ie} \times 3L^2 - 4a^2 \quad (2)$$

where Pa is the applied load (kN), a is the shear span or the distance between concentrated load and face of support (mm), Ec is the modulus of elasticity of concrete (MPa), and L is the span length of the beam. Ie, is the effective moment of inertia used in computing the deflection.

In Table 2, presented the calculation of theoretical moment and experimental moment is compared. This is done for SBN beams, CBN, CB. Furthermore, in Figure 11, the ultimate load (Pu), yielding load (Py), and first crack of the SBN, CBN, CB beam specimens. (Pcr).

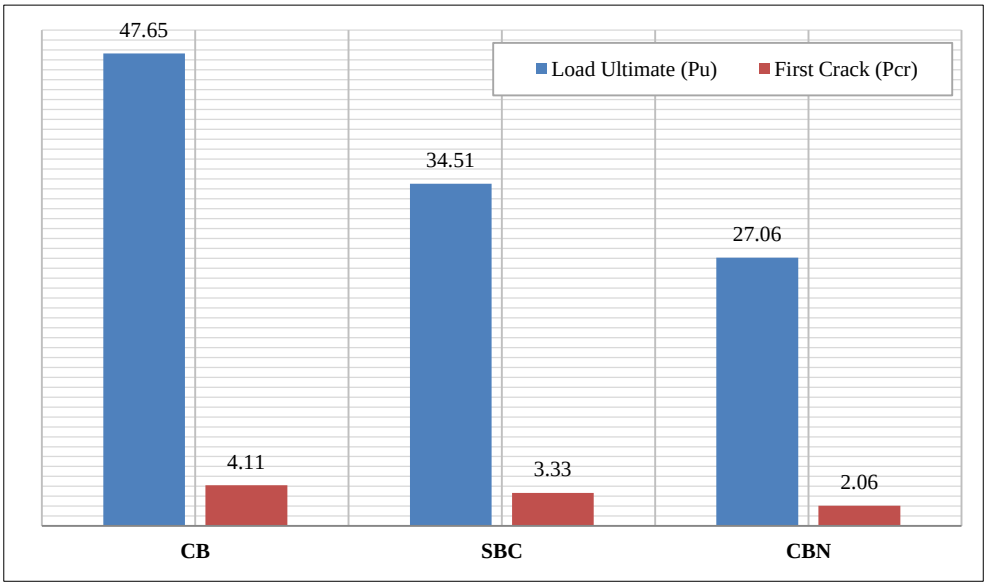

Figure 11. Comparison of loading capacity

The Specimen CB and CBN are beams with vertical shear reinforcement, while SCB uses spiral system shear reinforcement, as seen in Figure 11. CB and SCB ultimate capacities are 47.65 kN and 34.51 kN, respectively. This shows that the ultimate load (Pu) of the SCB beams was 27.57% lower than that of CB but 21.58% higher than the ultimate load (Pu) of CBN. Furthermore, the current experimental values are in close agreement with the previous works; compared with BRTP 60D. The ultimate load (Pu) SBN is similar to BTRP 60D and CBN Specimen, similar to BT [30]. Prediction of experimental ultimate load ratio and analysis, namely Mu exp / Mu cal calculation of the ratio of the capacity of the test result to the capacity of the moment of the theoretical result. The calculation results show that the capacity of the test result moment compared to the theoretical result moment has a ratio value of 0.80 to 1.3. Furthermore, the ultimate moment capacity obtained from the analytical method produced SBC lower, categorized as good.

3.2. Ultimate Flexural Capacity

Based on Figure 11, removing concrete in the concrete tension area of the beam on SBN and SBC causes a decrease in beam stiffness. This increases the deformation of the beam. As a result, the occurrence of the first crack was earlier in the CBN and SBN than (CB) control beams. The first cracks in the CBN, SBN and control (CB) beams occurred when the applied loads reached 2.06 kN, 3.33 and 4.11 kN, respectively. Initial crack (Pcr) of CBN beams is earlier than SBN beams, this is due to the change of conventional shear reinforcement model to spiral although it does not significantly increase the Pcr value of SBN beams.

3.3. Load-Strain of Concrete

Based on Figure 12, the concrete load graph drawing for SCB, Pcr beams occur when applied to a load of 3.33kN with a concrete strain of ε_c = 308.227 μ, while on CBN beams, there is a decrease in Pcr value, the beam has an initial crack when the load is applied by 2.06 with a concrete strain of 699 μ. An increase in Pcr load on SBC beams compared to CBN is possible by changing the sliding zinc reinforcement model from conventional to spiral. However, compared to control beams (CB), there was a decrease in Pcr load by 23.43%, and there was an increase in concrete strain by 36.56%. The increase in concrete loads is due to a reduction of the inertia of the beam due to the removal of concrete on the tensile cross-section. When the load is increased according to the level of the crack, a bending crack occurs. In this condition, it is assumed that the concrete has flexural cracks. Thus, the contribution of concrete tension can no longer exist, so the reinforcement of steel that holds it.

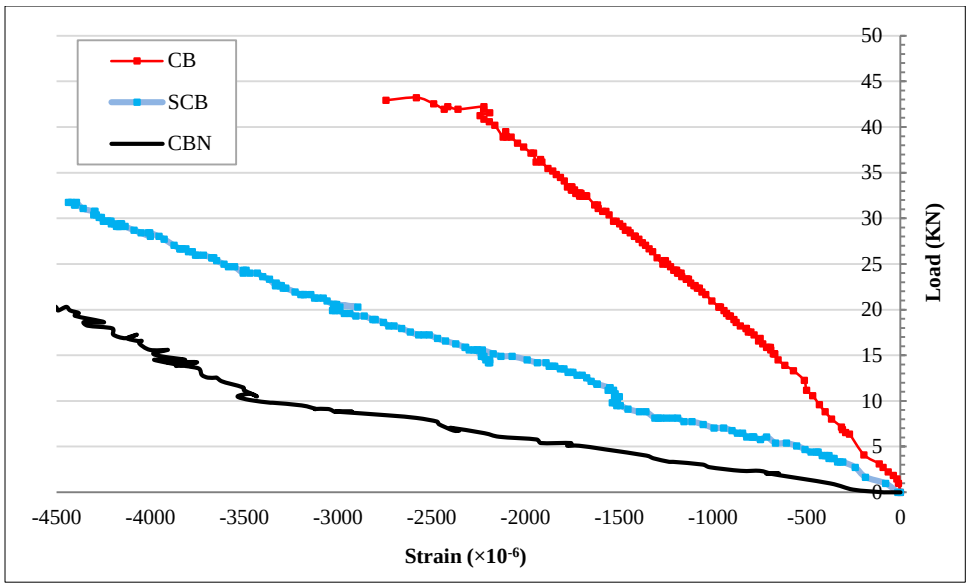

Figure 12. Load-Strain of concrete

3.4. Load- steel Reinforcement Strengthening Relation

The initial crack occurred on the CB beam with a load of 4.11 kN with a reinforcing strain of 11.13 kN. The ultimate load is 47.65 kN with a strain of 3608 μ. On the SBC Pcr beam, the initial crack occurred at a load of 3.33 kN with a strain of 155.26 μ, yielding a load of 33.82 with a strain of 1999.69 μ and an ultimate load of 34.51 kN with a strain of 2043.72 μ Furthermore, on the CBN specimen, the initial crack occurs at a load of 2.06 kN with a strain of 96.90 μ, yields reinforcement at a load of 25.68 kN with a strain of 1959.22, and ultimates at a load of 27.06 kN with a strain of 2110.8. It can be observed that there is a decrease in steel load and ductility in the SBC and CBN specimens. This can be observed from the behavior of the load-strain curve. The SBC and BCN specimens fail shortly after the main crossing melts. CB specimens can still deform before failure after the main reinforcement melts, in another case with CB specimens. If it is assumed that the steel strain yielding limit at the 2000μ strain, all the specimens yield reinforcement before the concrete is broken because it has a strain > 2000 μ. A graph of the load-strain relationship is shown in Figure 13.

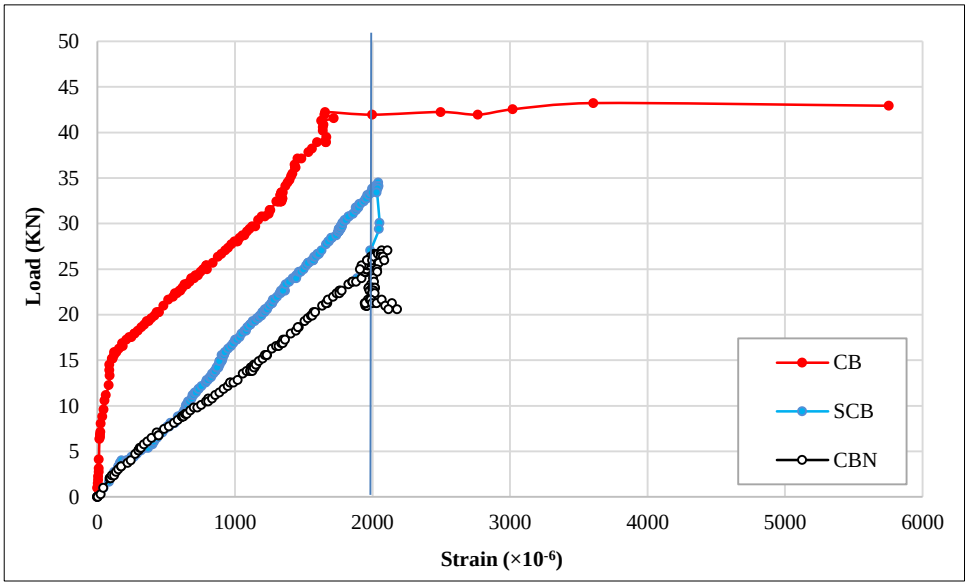

Figure 13. Load – of steel reinforcement

3.5. Behavior Crack Pattern

The cracking and collapse pattern in the CB beam is a failure of bending, with the spread of cracks propagating beyond 3/4 of the span of the beam. However, in specimens SBC and CBN, cracks indicate a transition from bending to sliding cracks, although dominated by flexural failure. This happens because the nominal shear strength of the concrete is still able to withstand the shear force that occurs on the beam, and the sliding crack that does not reach the loading point indicates that the zinc is holding the shear force well. The transition of the sliding failure is getting more significant

and more noticeable as the load is applied. Figure 14 shows that the strain of the transverse reinforcement in the SBC specimen is greater than the control beam (CB) strain. Even though the transverse reinforcement has not decayed during the ultimate load, it is smaller than the strain of the shear reinforcement in the CBN specimen. The transverse reinforcement has melted before the ultimate load.

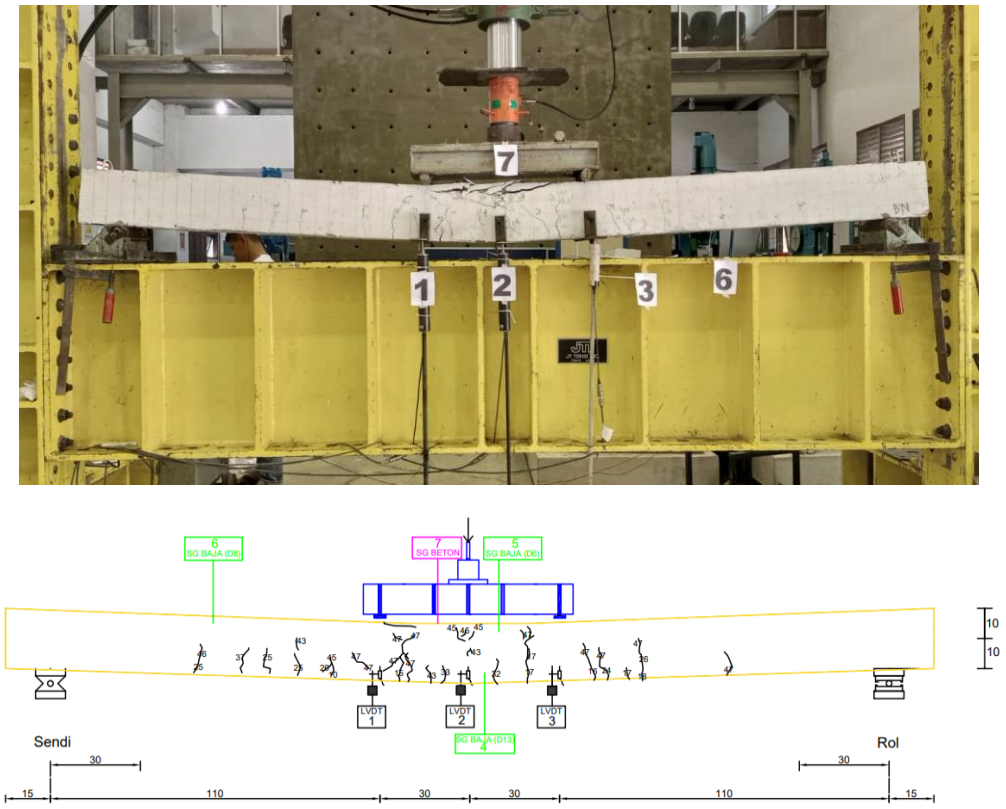

(a) Crack pattern specimen CB

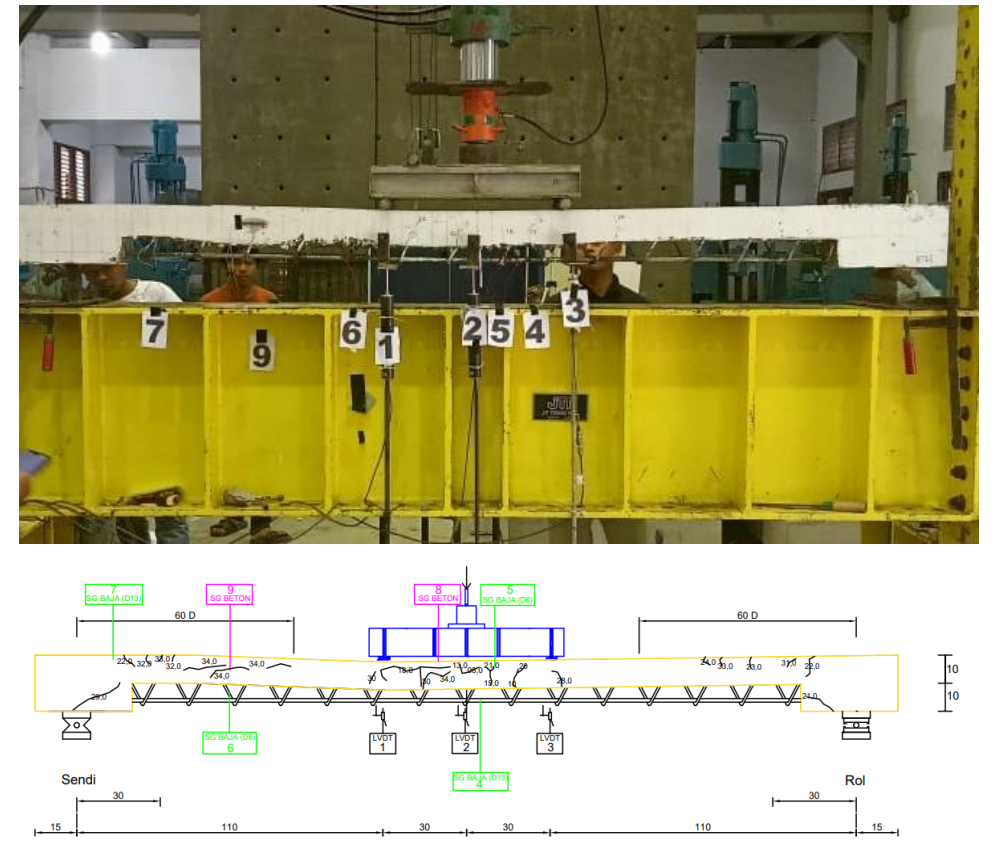

(b) Crack pattern Specimen SCB

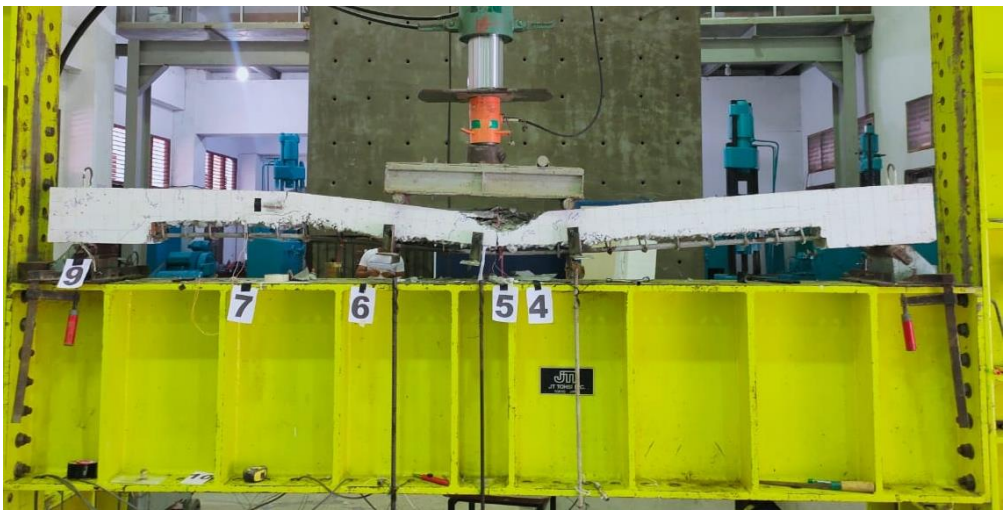

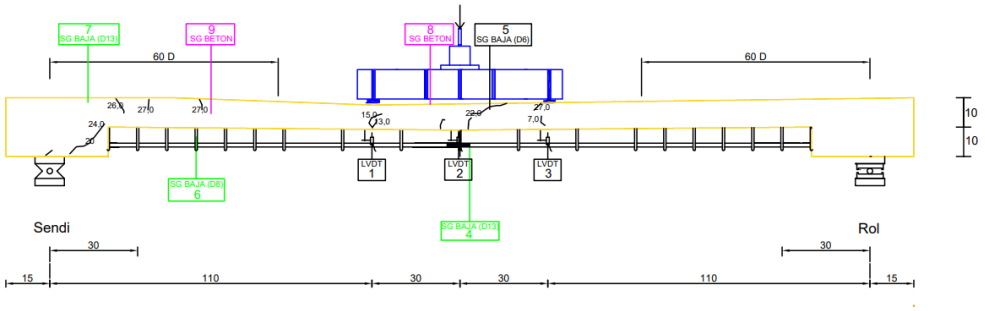

(c) Crack pattern specimen SBN

Figure 14. Crack Pattern specimens CB, SCB, CBN

4. Conclusion

The first crack load on the SCB beam is higher than the CBN beam, and the deflection is lower, but compared to the control beam (NB), the first crack of the SBC specimen is lower. This indicates that the beam does not yet have enough tenacity in the elastic phase compared to the control beam. The ultimate capacities of CB and SCB are 47.65 kN and 34.51 kN, respectively. This shows that the maximum load (Pu) of the SCB beam decreased by 27.57% compared to the CB. This is possible by the decrease in inertia in the beam SBC but increased by 21.58% compared to the ultimate load of CBN (Pu) due to the change of the shear rebar model from vertical geometry to spiral, where this spiral rebar can increase the bending capacity of the beam, similar with the BTRP 60D using truss system reinforcement can also increase the bending capacity of the beam. There is a bending crack in the CB beam, while in SBC and CBN it has shear-bending cracks. All the beams suffered under reinforced failure. Failure was initiated by the yielding of steel reinforcement and is followed by compression failure in concrete. Concrete-less beams in the tension section can reduce the use of concrete, and the weight of the beam decreased by 38.16% but experienced a decrease in the bending capacity compared to CB. SBN is better compared to CBN beams in terms of ultimate load and ductility and has an ultimate service load that is almost the same as BTRP 60D, so more research is needed to develop, confirm, and expand the findings in this study in terms of some experimental variation models and reinforcing of the beams.

5. Declarations

5.1. Author Contributions

Conceptualization, A.A.; methodology, A.A., L.O., and F.I.; software, F.I.; validation, A.A.; investigation, L.O. and F.I.; data curation, A.A.; writing—original draft preparation, A.A. and F.I.; writing—review and editing, A.A. and F.I.; supervision, A.A. All authors have read and agreed to the published version of the manuscript.

5.2. Data Availability Statement

The data presented in this study are available on request from the corresponding author.

5.3. Funding

The researcher acknowledges that this research can be achieved with the financial support of Internal Grants from Teuku Umar University.

5.4. Acknowledgements

The researcher acknowledges that this research can be achieved with the financial support of Teuku Umar University (Institution of Education Fund Management). Also, to students and staff of the Laboratory of Materials and Structures at Syiah Kuala University.

5.5. Conflicts of Interest

The authors declare no conflict of interest.

6. References

[1] Gerges, N. N., Issa, C. A., Sleiman, E., Aintrazi, S., Saadeddine, J., Abboud, R., & Antoun, M. (2022). Eco-Friendly Optimum Structural Concrete Mix Design. Sustainability (Switzerland), 14(14). doi:10.3390/su14148660.

[2] Prabha, S. L., Surendar, M., & Neelamegam, M. (2019). Experimental investigation of eco-friendly mortar using industrial wastes. Journal of Green Engineering, 9(4), 626–637.

[3] Elsayed, M., Tayeh, B. A., Abu Aisheh, Y. I., El-Nasser, N. A., & Elmaaty, M. A. (2022). Shear strength of eco-friendly self-compacting concrete beams containing ground granulated blast furnace slag and fly ash as cement replacement. Case Studies in Construction Materials, 17, e01354. doi:10.1016/j.cscm.2022.e01354.

[4] Balaji, G., & Vetturayasudharsanan, R. (2020). Experimental investigation on flexural behaviour of RC hollow beams. Materials Today: Proceedings, 21, 351–356. doi:10.1016/j.matpr.2019.05.461.

[5] Ismael, M. A., & Hameed, Y. M. (2022). Structural behavior of hollow-core reinforced self-compacting concrete beams. SN Applied Sciences, 4(5). doi:10.1007/s42452-022-05036-6.

[6] Hassan, N. Z., Ismael, H. M., & Salman, A. M. (2018). Study Behavior of Hollow Reinforced Concrete Beams. International Journal of Current Engineering and Technology, 8(6), 1640–1651.

[7] Kanna, M.D., & Arun, M. (2021). Effects of Longitudinal and Transverse Direction Opening in Reinforced Concrete Beam: The State of Review. IOP Conference Series: Materials Science and Engineering, 1059(1). doi:10.1088/1757-899X/1059/1/012049.

[8] Manikandan, S., Dharmar, S., & Robertravi, S. (2015). Experimental study on flexural behaviour of reinforced concrete hollow core sandwich beams. International Journal of Advance Research in Science and Engineering, 4(01), 937-946.

[9] Patel, R. R. (2018). Flexural Behavior and Strength of Doubly-Reinforced Concrete Beams with Hollow Plastic Spheres. Old Dominion University, Norfolk, United States.

[10] Ataria, R. B., & Wang, Y. C. (2019). Bending and shear behaviour of two layer beams with one layer of rubber recycled aggregate concrete in tension. Structures, 20, 214–225. doi:10.1016/j.istruc.2019.03.014.

[11] Syahrul, S., Tjaronge, M. W., Djamaluddin, R., & Amiruddin, A. A. (2021). Flexural Behavior of Normal and Lightweight Concrete Composite Beams. Civil Engineering Journal, 7(3), 549–559. doi:10.28991/cej-2021-03091673.

[12] Fakhruddin, Irmawaty, R., & Djamaluddin, R. (2022). Flexural behavior of monolith and hybrid concrete beams produced through the partial replacement of coarse aggregate with PET waste. Structures, 43, 1134–1144. doi:10.1016/j.istruc.2022.07.015.

[13] Hussein, L. F., Khattab, M. M., & Farman, M. S. (2021). Experimental and finite element studies on the behavior of hybrid reinforced concrete beams. Case Studies in Construction Materials, 15, e00607. doi:10.1016/j.cscm.2021.e00607.

[14] Djamaluddin, R. (2013). Flexural behaviour of external reinforced concrete beams. Procedia Engineering, 54, 252–260. doi:10.1016/j.proeng.2013.03.023.

[15] Amir, A., Djamaluddin, R., Irmawati, R., & Amiruddin, A. A. (2020). Effect steel reinforcement ratio on the behavior of RC beam without concrete at tension zone using truss-system reinforcement. IOP Conference Series: Earth and Environmental Science, 419(1). doi:10.1088/1755-1315/419/1/012050.

[16] Vatulia, G., Komagorova, S., & Pavliuchenkov, M. (2018). Optimization of the truss beam. Verification of the calculation results. MATEC Web of Conferences, 230, 02037. doi:10.1051/matecconf/201823002037.

[17] Afefy, H., Taher, S., Fawzy, O., & Salem, S. (2022). Numerical Simulation of RC Beams Reinforced with Internal Steel Trusses. International Journal of Advances in Structural and Geotechnical Engineering, 03(02), 38–51. doi:10.21608/asge.2022.152826.1023.

[18] Tarawneh, A., Almasabha, G., Alawadi, R., & Tarawneh, M. (2021). Innovative and reliable model for shear strength of steel fibers reinforced concrete beams. Structures, 32, 1015–1025. doi:10.1016/j.istruc.2021.03.081.

[19] Elansary, A. A., Elnazlawy, Y. Y., & Abdalla, H. A. (2022). Shear behaviour of concrete wide beams with spiral lateral reinforcement. Australian Journal of Civil Engineering, 20(1), 174–194. doi:10.1080/14488353.2021.1942405.

[20] Saha, P., & Meesaraganda, L. V. P. (2019). Experimental investigation of reinforced SCC beam-column joint with rectangular spiral reinforcement under cyclic loading. Construction and Building Materials, 201, 171–185. doi:10.1016/j.conbuildmat.2018.12.192.

[21] Ibrahim, A., Askar, H. S., & El-Zoughiby, M. E. (2022). Torsional behavior of solid and hollow concrete beams reinforced with inclined spirals. Journal of King Saud University - Engineering Sciences, 34(5), 309–321. doi:10.1016/j.jksues.2020.10.008.

[22] Askandar, N. H., & Mahmood, A. D. (2020). Torsional Strengthening of RC Beams with Continuous Spiral Near-Surface Mounted Steel Wire Rope. International Journal of Concrete Structures and Materials, 14(1). doi:10.1186/s40069-019-0386-4.

[23] Ibrahim, A., Askar, H. S., & El-Zoughiby, M. E. (2022). Experimental and Numerical Nonlinear Analysis of Hollow RC Beams Reinforced with Rectangular Spiral Stirrups under Torsion. Iranian Journal of Science and Technology - Transactions of Civil Engineering, 46(6), 4019–4029. doi:10.1007/s40996-022-00852-7.

[24] Al-Faqra, E., Murad, Y., Abdel Jaber, M., & Shatarat, N. (2021). Torsional behaviour of high strength concrete beams with spiral reinforcement. Australian Journal of Structural Engineering, 22(4), 266–276. doi:10.1080/13287982.2021.1962489.

[25] Shatarat, N., Mahmoud, H. M., & Katkhuda, H. (2018). Shear capacity investigation of self-compacting concrete beams with rectangular spiral reinforcement. Construction and Building Materials, 189, 640–648. doi:10.1016/j.conbuildmat.2018.09.046.

[26] Azimi, M., Campos, U. A., Matthews, J. C., Lu, H., Tehrani, F. M., Sun, S., & Alam, S. (2020). Experimental and Numerical Study of Cyclic Performance of Reinforced Concrete Exterior Connections with Rectangular-Spiral Reinforcement. Journal of Structural Engineering, 146(3), 4019219. doi:10.1061/(asce)st.1943-541x.0002506.

[27] ACI 211.2-98. (2004). Standard Practice for Selecting proportionds for Structural Lightweight Concrete (ACI 211.2-98). American Concrete Institute (ACI), Farmington Hills, United States.

[28] ASTM C33-03. (2010). Standard Specification for Concrete Aggregates. ASTM International, Pennsylvania, United States. doi:10.1520/C0033-03.

[29] ASTM C39/C39M-03. (2017). Standard Test Method for Compressive Strength of Cylindrical Concrete Specimens. ASTM International, Pennsylvania, United States. doi:10.1520/C0039_C0039M-03.

[30] Narule, G. N., & Sonawane, K. K. (2022). Flexural and shear cracking performance of strengthened RC rectangular beam with variable pattern of the BFRP strips. Innovative Infrastructure Solutions, 7(2), 1-16. doi:10.1007/s41062-022-00785-0.